PO Box 2345, Beijing 100023, China
www.wjgnet.com
wjg@wjgnet.com

World J Gastroenterol 2006 June 21; 12(23): 3756-3759
World Journal of Gastroenterology ISSN 1007-9327

RAPID COMMUNICATION

Risk factors for retinopathy associated with interferon α-2b and ribavirin combination therapy in patients with chronic hepatitis C

Chiaki Okuse, Hiroshi Yotsuyanagi, Yoshihiko Nagase, Yuhtaro Kobayashi, Kiyomi Yasuda, Kazuhiko Koike, Shiro Iino, Michihiro Suzuki, Fumio Itoh

Chiaki Okuse, Yoshihiko Nagase, Yuhtaro Kobayashi, Michihiro Suzuki, Fumio Itoh, Division of Gastroenterology and Hepatology, Department of Internal Medicine, St. Marianna University School of Medicine, Kawasaki, Kanagawa, 216-8511, Japan
Hiroshi Yotsuyanagi, Kazuhiko Koike, Department of Infectious Diseases, Internal Medicine, Faculty of Medicine, University of Tokyo, 7-3-1, Hongo, Bunkyo, Tokyo 113-8655, Japan
Kiyomi Yasuda, Shiro Iino, Center for Liver Diseases, Kiyokawa Hospital, Minamiasagaya, Suginami, Tokyo, 166-0004, Japan
Correspondence to: Dr. Hiroshi Yotsuyanagi, Department of Infectious Diseases, Internal Medicine, Faculty of Medicine, University of Tokyo, 7-3-1, Hongo, Bunkyo, Tokyo 113-8655, Japan. hyotsu-tky@umin.ac.jp
Telephone: +81-3-58008720 Fax: +81-3-58008796
Received: 2006-01-13 Accepted: 2006-02-18

Abstract

AIM: To elucidate the frequency and risk factors for retinopathy in patients with chronic hepatitis C who are treated by interferon-ribavirin combination therapy.

METHODS: We prospectively analyzed 73 patients with histologically confirmed chronic hepatitis C, who underwent combination therapy for 24 wk. Optic fundi were examined before, and 2, 4, 12 and 24 wk after the start of combination therapy.

RESULTS: Fourteen patients (19%) developed retinopathy, which was initially diagnosed by the appearance of a cotton wool spot in 12 patients. Retinal hemorrhage was observed in 5 patients. No patient complained of visual disturbance. Retinopathy disappeared in 9 patients (64%) despite the continuation of combination therapy. However, retinopathy persisted in 5 patients with retinal hemorrhage. A comparison of the clinical background between the groups with and without retinopathy showed no significant differences in age, gender, viral genotype, RNA level, white blood cell count, platelet count, prothrombin time, complications by diabetes mellitus or hypertension, or pretreatment arteriosclerotic changes in the optic fundi. However, multiple logistic regression analysis revealed that complication by hypertension was observed with a high frequency in the group with retinopathy (P = 0.004, OR = 245.918, 95% CI = 5.6-10786.2).

CONCLUSION: Retinopathy associated with combination therapy of interferon α-2b and ribavirin tends to develop in patients with hypertension.

Key words: Retinopathy; Ribavirin; Chronic hepatitis C; Interferon

Okuse C, Yotsuyanagi H, Nagase Y, Kobayashi Y, Yasuda K, Koike K, Iino S, Suzuki M, Itoh F. Risk factors for retinopathy associated with interferon α-2b and ribavirin combination therapy in patients with chronic hepatitis C.*World J Gastroenterol* 2006; 12(23): 3756-3759

http://www.wjgnet.com/1007-9327/12/3756.asp

INTRODUCTION

Chronic hepatitis C, which affects more than 170 million people in the world[1], may eventually lead to cirrhosis and/or hepatocellular carcinoma. The main treatment for this intractable disease is interferon administration. Published guidelines recommend interferon-ribavirin combination therapy as a first-line treatment[2]. Interferon is also used in the treatment of other viral and neoplastic diseases.

Various adverse effects have been reported due to use of interferon[3]. An influenza-like syndrome, characterized by fever, chills, myalgias, arthralgias, and headache, is the most common adverse effect. Toxicities of the central nervous, hematopoietic, gastrointestinal, urinary, cardiovascular, musculoskeletal and endocrine systems have also been described. However, ocular toxicity was not reported before the use of interferon for chronic hepatitis[3].

After the introduction of interferon for the treatment of hepatitis, retinal complications have been reported. Hayakawa *et al* showed that 17 of 43 patients developed retinopathy during interferon monotherapy. They also showed that the prevalence of retinopathy was higher in patients with diabetes[4]. Subsequently, several papers have shown that a substantial proportion of patients undergoing interferon monotherapy develop retinopathy[5-7]. However, the prevalence of retinopathy is variable, which is

presumably attributed to the difference in the treatment regimen and/or background of patients.

As mentioned above, interferon-ribavirin combination therapy has become the standard treatment for chronic hepatitis C. Results from recent studies have suggested that the prevalence of retinopathy associated with combination therapy may be higher than that associated with interferon monotherapy, which should be further investigated[8-10].

In spite of the high prevalence, risk factors for interferon-associated retinopathy are still unclear. Diabetes mellitus and the patients' age were reported to be possible risk factors for retinopathy associated with interferon monotherapy[4]. In interferon-ribavirin combination therapy, diabetes, hypertension[8], and response to treatment[10] were considered possible risk factors. However, the results are not conclusive because of the small number of patients examined.

The aim of the present study is to elucidate the prevalence and risk factors for retinopathy associated with interferon-ribavirin combination therapy.

MATERIALS AND METHODS

Patients

Seventy-three consecutive patients with histologically confirmed chronic hepatit is C (47 males and 26 females; median age, 53.4 years; ranges 26-73 years) were enrolled in this study from 2002 to 2004. The clinical backgrounds of the enrolled patients are shown in Table 1. All patients were treated with recombinant interferon α-2b (Intron A, Schering-Plough, Kenilworth, NJ, USA) and ribavirin (Rebetol; Schering-Plough, Kenilworth, NJ, USA) combination therapy. All the patients were treated daily with interferon α-2b at 6 MU for 2 wk followed by three times a wk treatment with interferon α-2b at 6 MU for 22 wk in combination with ribavirin. Ribavirin was given orally twice a day at a total daily dose of 600 mg for patients who weighed 60 kg or less and 800 mg for the remaining patients who weighed more than 60 kg for 24 wk.

All patients were assessed to determine the safety, tolerance, and efficacy of the treatment at the end of wk 1, 2, 4, and every 4 wk during the treatment. After the treatment was completed, patients were followed up on wk 4, 8, 12, and 24. The primary end point was indicated by a sustained loss of detectable HCV-RNA at 24 wk after the treatment.

Methods

Optic fundi were examined before, and 2, 4, 12 and 24 wk after the start of combination therapy. Ophthalmological examinations were carried out before the start of treatment and 2, 4, 12 and 24 wk after the start of treatment until the completion of treatment or until the retinopathy disappeared. Fundus photographs were taken for documentation and comparison when retinal abnormalities were detected.

Informed consent was obtained from each patient. The study protocol conformed to the ethical guidelines of the 1975 Declaration of Helsinki and was approved by the Ethics Committees of our institutions.

Table 1 Profiles and initial laboratory data of patients with and without retinopathy during IFN-ribavirin combination therapy[1]

	Total	Retinopathy (+)	Retinopathy (-)
Patients			
Number	73	14	59
Age (yr)	53.4 ± 10.9	56.3 ± 10.5	52.8±38.6
Gender (M/F)	47/26	10/4	37/22
Hypertension (Yes/No)[a]	15/58	5/8	10/49
Diabetes mellitus (Yes/No)	2/71	1/13	1/58
Peripheral blood count			
Platelet count ($\times 10^4/mm^3$)	15.3 ± 6.0	12.5 ± 10.5	15.9 ± 38.6
White blood cell ($\times 10^3/mm^3$)	46.9 ± 12.6	46.5 ± 13.0	48.6 ± 10.9
Hemoglobin (×g/dL)	14.0 ± 1.3	14.0 ± 1.0	14.0 ± 1.4
Prothrombin time (%)	90.2 ± 13.3	87.1 ± 13.3	90.8 ± 13.3
ALT (IU/L)	109.4 ± 78.2	104.1 ± 41.0	110.4 ± 83.6
Viral factors			
Genotype (type 1/type 2)[2]	45/26	33/24	12/2
Viral load (kcopies/mL)	592.3 ± 271.2	505.6 ± 309.1	607.5 ± 271.2
Pretreatment/ Arteriosclerotic	12/61	7/7	5/54
changes in optic fundi (Yes/No)			
Response to therapy (SVR/non-SVR)	38/35	5/9	33/26

[1] Data are expressed as mean ± SD.
[2] Genotype could not be determined in 2 patients.
[a] $P = 0.004$

RESULTS

Before the start of the combinaiton therapy, one patient had scars from laser coagulation of a previous interferon-associated retinopathy and another patient had retinal central vein occlusion. Arteriosclerotic changes of the optic fundi were observed in 12 patients.

After the start of interferon-ribavirin combination therapy, 14 out of 73 patients (19%) developed retinopathy. The clinical profiles and laboratory data of the patients with and without retinopathy are shown in Table 1.

We compared the characteristics of patients who developed retinopathy and those who did not. The two groups showed no statistical differences in age, gender, subtype of virus, RNA level, white blood cell count, platelet count, prothrombin time before treatment or prevalence of pretreatment fundic arteriosclerotic changes. The patients with retinopathy were more frequently complicated by hypertension ($P = 0.004$) (Table 1).

Logistic regression analysis of factors affecting retinopathy was also carried out. Hypertension was found to be a factor for predicting retinopathy (Table 2).

Table 3 shows the optic fundi findings of the 14 patients with retinopathy. Retinopathy was initially diagnosed by the appearance of a cotton wool spot in 12 patients. In three of the 12 patients, retinal hemorrhage was also observed simultaneously or sequentially. Two of the 14 patients who developed retinopathy were diagnosed by retinal hemorrhage without a cotton wool spot. No patient complained of the visual disturbance.

Table 2 Logistic regression analysis of factors associated with retinopathy

Factor	*P*	Odds ratio	95% confidence interval
Sex	0.68	1.699	0.1-21.0
Age	0.203	1.099	1.0-1.3
Genotype	0.776	1.621	0.1-45.5
Levels of HCV RNA	0.114	1.006	0.99-1.0
Hypertension	0.004	246.32	5.5-10977.8
Diabetes mellitus	0.211	0.122	0.1-3.3
Abnormal findings in pretreatment optic fundi	0.904	1.192	0.1-20.3
Platelet	0.059	1.391	1.0-1.9
Prothrombin time	0.747	0.982	0.9-1.1
ALT	0.992	1	0.98-1.0
WBC	0.964	1.027	0.4-2.9
Response to therapy (SVR or non-SVR)	0.123	0.016	0.0-3.1

Table 3 Optic fundi findings of patients with retinopathy

No	Age	Sex	Underlying disease		Optic fundi before treatment		Optic fundi after treatment	
			Hyper tension	Diabetes mellitus	H	S	Cotton wool spot	Retinal hemorrhage
1	38	M	+	+	0	0	4 wk-	4 wk-
2	52	M	+	-	1	0	4-12 wk	-
3	40	M	-	-	0	0	6-36 wk	-
4	62	F	-	-	0	0	4-36 wk	-
5	61	M	+	-	0	0	12 wk-	-
6	58	M	-	-	1	1	12 wk-	-
7	73	M	-	-	2	2	4-28 wk	-
8	65	F	+	-	0	0	24-36 wk	-
9	59	F	+	-	2	2	2 wk-	4-24 wk
10	40	M	-	-	0	0	4-20 wk	-
11	62	F	-	-	1	2	2 wk-	4 wk-
12	65	M	-	-	1	1	2-24 wk	-
13	40	M	-	-	0	0	-	8-16 wk
14	40	M	-	-	0	0	-	2-4 wk

Retinopathy disappeared in 9 of the 14 patients despite the continuation of combination therapy. However, it continued in three patients with retinal hemorrhage and two without retinal hemorrhage.

Ocular manifestations other than retinopathy (e.g., ocular pain, a mild watery eye and conjunctivitis) were not observed in any patients.

DISCUSSION

Interferon associated retinopathy was first recognized in 1990 when Ikebe and associates reported a 39-year-old patient who developed retinal hemorrhages and cotton wool spots following intravenous administration of interferon[11].

The exact mechanism of interferon-induced-retinopathy is not known but is presumably related to the disturbance in retinal microcirculation[12]. Therefore, preexisting arteriosclerosis that affects microcirculation may promote interferon-induced retinopathy.

Our study shows that hypertension is a more frequent complication in patients with interferon-induced-retinopathy. Chronic hypertension is associated with the thickening of the walls of the arteries and small arterioles[13]. Therefore, systemic hypertension predisposes patients to interferon-induced-retinopathy. The fact that hypertensive retinopathy induces the formation of flame-shaped hemorrhages and white cotton wool spots, which are also seen in interferon-induced-retinopathy, implies that systemic hypertension and interferon-induced-retinopathy may be related each other.

Statistical analysis did not indicate pretreatment optic fundic changes or diabetes as predictive factors of retinopathy. This may be attributed to the following reasons: (1) pretreatment changes in the optic fundi as a predictive factor are included in hypertension; and (2) the number of patients with diabetes is too small. Regardless of these reasons, systemic hypertension is an important risk factor for interferon-related retinopathy.

The frequencies of interferon-induced retinopathy associated with interferon monotherapy and interferon-ribavirin combination therapy are reported to be 24%-58%[4-7,14,15] and 16%-64%[8-10,16], respectively. The frequency in the present study (20%) was lower than that in previous reports. Furthermore, the ocular side effects of ribavirin, which include a mild watery eye and conjunctivitis, were not seen in this study. Therefore, the frequency of induced retinopathy associated with combination therapy may be considered as high as that associated with interferon monotherapy.

Retinopathy developed by 12 wk in most (13/14, 93%) of the patients after the start of combination therapy and disappeared in majority (10/14, 71%) of the patients during the 4-8 wk period, in which the patients were receiving the treatment. This suggests that treatment can be continued despite the development of retinopathy in many patients. However, two patients who developed cotton wool spots early in the therapy (2 wk) therafter suffered from retinal hemorrhage in a prolonged manner. Therefore, patients who develop cotton wool spots early in the therapy should be carefully monitored. However, as reported in previous studies[4,8,17], most of the patients with retinopathy in this study were asymptomatic. Therefore, combination therapy may be continued in most patients.

The fact that retinopathy occurred more frequently in patients with hypertension, suggests that these patients should be carefully monitored. With periodic examination of the optic fundi, major bleeding that causes visual symptoms may be prevented or detected at an early stage. Therefore, patients who undergo interferon-ribavirin combination therapy, particularly those with hypertension, should undergo periodic examination of the optic fundi.

To conclude, retinopathy associated with combination therapy of interferon α-2b and ribavirin tends to develop in patients with hypertension.

REFERENCES

1 Hepatitis C-global prevalence (update). Wkly Epidemiol Rec 1999; 74: 425-427

2 **Strader DB**, Wright T, Thomas DL, Seeff LB. Diagnosis, management, and treatment of hepatitis C. *Hepaology* 2004; **39**: 1147-1171
3 **Quesada JR**, Talpaz M, Rios A, Kurzrock R, Gutterman JU. Clinical toxicity of interferons in cancer patients: a review. *J Clin Oncol* 1986; **4**: 234-243
4 **Hayasaka S**, Fujii M, Yamamoto Y, Noda S, Kurome H, Sasaki M. Retinopathy and subconjunctival haemorrhage in patients with chronic viral hepatitis receiving interferon alfa. *Br J Ophthalmol* 1995; **79**: 150-152
5 **Sugano S**, Suzuki T, Watanabe M, Ohe K, Ishii K, Okajima T. Retinal complications and plasma C5a levels during interferon alpha therapy for chronic hepatitis C. *Am J Gastroenterol* 1998; **93**: 2441-2444
6 **Kawano T**, Shigehira M, Uto H, Nakama T, Kato J, Hayashi K, Maruyama T, Kuribayashi T, Chuman T, Futami T, Tsubouchi H. Retinal complications during interferon therapy for chronic hepatitis C. *Am J Gastroenterol* 1996; **91**: 309-313
7 **Saito H**, Ebinuma H, Nagata H, Inagaki Y, Saito Y, Wakabayashi K, Takagi T, Nakamura M, Katsura H, Oguchi Y, Ishii H. Interferon-associated retinopathy in a uniform regimen of natural interferon-alpha therapy for chronic hepatitis C. *Liver* 2001; **21**: 192-197
8 **Cuthbertson FM**, Davies M, McKibbin M. Is screening for interferon retinopathy in hepatitis C justified? *Br J Ophthalmol* 2004; **88**: 1518-1520
9 **Schulman JA**, Liang C, Kooragayala LM, King J. Posterior segment complications in patients with hepatitis C treated with interferon and ribavirin. *Ophthalmology* 2003; **110**: 437-442
10 **Jain K**, Lam WC, Waheeb S, Thai Q, Heathcote J. Retinopathy in chronic hepatitis C patients during interferon treatment with ribavirin. *Br J Ophthalmol* 2001; **85**: 1171-1173
11 **Ikebe T**, Nakatsuka K and Goto M. A case of retinopathy induced by intravenous administration of interferon. *Folia Ophthalmol Jpn (Ganka-Kiyo)* 1990; **41**: 2291-2296 (in Japanese)
12 **Guyer DR**, Yannuzzi LA, Chang S, Shields JA, Green WR. Rerina-Vitreous-Macula. 1st ed. Philadelphia: W.B. Saunders, 1999: 864
13 **Sharrett AR**, Hubbard LD, Cooper LS, Sorlie PD, Brothers RJ, Nieto FJ, Pinsky JL, Klein R. Retinal arteriolar diameters and elevated blood pressure: the Atherosclerosis Risk in Communities Study. *Am J Epidemiol* 1999; **150**: 263-270
14 **Hejny C**, Sternberg P, Lawson DH, Greiner K, Aaberg TM Jr. Retinopathy associated with high-dose interferon alfa-2b therapy. *Am J Ophthalmol* 2001; **131**: 782-787
15 **Kadayifcilar S**, Boyacioglu S, Kart H, Gursoy M, Aydin P. Ocular complications with high-dose interferon alpha in chronic active hepatitis. *Eye* 1999; **13** (Pt 2): 241-246
16 **Chisholm JA**, Williams G, Spence E, Parks S, Keating D, Gavin M, Mills PR. Retinal toxicity during pegylated alpha-interferon therapy for chronic hepatitis C: a multifocal electroretinogram investigation. *Aliment Pharmacol Ther* 2005; **21**: 723-732
17 **Guyer DR**, Tiedeman J, Yannuzzi LA, Slakter JS, Parke D, Kelley J, Tang RA, Marmor M, Abrams G, Miller JW. Interferon-associated retinopathy. *Arch Ophthalmol* 1993; **111**: 350-356

S- Editor Pan BR **E- Editor** Liu Y

+ Model

Available online at www.sciencedirect.com
SCIENCE DIRECT®

Antiviral Research xxx (2006) xxx–xxx

Antiviral Research
www.elsevier.com/locate/antiviral

Cooperative contribution of gag substitutions to nelfinavir-dependent enhancement of precursor cleavage and replication of human immunodeficiency virus type-1

Saori Matsuoka-Aizawa [a,b], Hiroyuki Gatanaga [a,*], Hironori Sato [c], Kazuhiko Koike [b], Satoshi Kimura [a], Shinichi Oka [a]

[a] *AIDS Clinical Center, International Medical Center of Japan, 1-21-1, Toyama, Shinjuku-ku, Tokyo 162-8655, Japan*
[b] *Graduate School of Medicine, University of Tokyo, Japan*
[c] *Division of Molecular Genetics, National Institute of Infectious Diseases, Tokyo, Japan*

Received 9 June 2005; accepted 11 January 2006

Abstract

We previously described a clinical human immunodeficiency virus type-1 (HIV-1) isolate, CL-4, which showed nelfinavir (NFV)-dependent enhancement of replication (Matsuoka-Aizawa, S., Sato, H., Hachiya, A., Tsuchiya, K., Takebe, Y., Gatanaga, H., Kimura, S., Oka, S, 2003. Isolation and molecular characterization of a nelfinavir (NFV)-resistant human immunodeficiency virus type 1 that exhibits NFV-dependent enhancement of replication. J. Virol. 77, 318–327.). To identify the responsible region(s) of HIV-1 proteins for such replication enhancement, we constructed a panel of recombinant HIV-1 clones harboring portions of the Gag and protease of CL-4 and analyzed their replication capabilities and Gag processing patterns. Our data suggested that the substitutions in the matrix and N-terminal half of capsid of CL-4 were indispensable for the NFV-dependent enhancement of replication and that NFV facilitated the cleavage between the matrix and capsid of the Gag precursor harboring these substitutions. The substitutions in C-terminal half of capsid rather decreased the cleavability of Gag precursor and NFV counteracted such negative impact. Efficient replication enhancement with NFV can be observed only in the presence of the substitutions in entire Gag and protease of CL-4.

Keywords: Human immunodeficiency virus type 1; Nelfinavir-resistant; Gag mutation

1. Introduction

Under the selective pressure of antiretroviral agents, the human immunodeficiency virus type-1 (HIV-1) evolves and acquires drug-resistance-associated mutations. The major protease inhibitor (PI)-resistance-associated mutations are located in the active sites of HIV-1 protease and impair its enzymatic functions (Bleiber et al., 2001; Croteau et al., 1997; Martinez-Picado et al., 1999). In order to compensate such impaired enzymatic function, PI-resistant HIV-1 further acquires mutations not only in protease but also in one of its substrate, Gag, resulting in full recovery of replication ability (Doyon et al., 1996; Gatanaga et al., 2002; Tamiya et al., 2004; Zhang et al., 1997). We previously described a unique clinical HIV-1 isolate, CL-4, which replicated more efficiently in the presence of sub-inhibitory concentrations of nelfinavir (NFV) (0.001–0.1 μM) (Matsuoka-Aizawa et al., 2003). CL-4 had a total of 56 amino acid substitutions in *gag-pro* genes compared with NL4-3; 22 substitutions had emerged in the matrix, SP1, and protease during administration of NFV-containing therapy, and 34 other substitutions had already existed before the introduction of the therapy (Matsuoka-Aizawa et al., 2003). In that study, we constructed three HIV-1 clones including, p17PRmt, PRmt, and p24PRmt, and found that only p17PRmt, which possessed the entire Gag and protease segment of CL-4, showed NFV-dependent enhancement of replication. Therefore, we concluded that the substitutions in matrix are indispensable for replication enhancement (Matsuoka-Aizawa et al., 2003). However, it is still unknown whether the substitutions in matrix alone are sufficient or whether other Gag substitutions are necessary for the replication enhancement with NFV. In this study we constructed four more recombinant HIV-1 clones and characterized their replica-

* Corresponding author. Tel.: +81 3 5273 5193; fax: +81 3 5273 5193.
E-mail address: higatana@imcj.acc.go.jp (H. Gatanaga).

0166-3542/$ – see front matter © 2006 Elsevier B.V. All rights reserved.
doi:10.1016/j.antiviral.2006.01.004

tion kinetics and Gag processing in the absence and presence of NFV.

2. Materials and methods

2.1. Cells and antiretroviral agents

HeLa cells were maintained in Dulbecco's minimal essential medium (DMEM) supplemented with 10% fetal calf serum (FCS). Transformed T cell lines, MT-2, PM-1, and H9 cells were maintained in RPMI-1640 with 10% FCS. NFV was kindly provided by the Japan Tobacco Co. (Tokyo, Japan).

2.2. Plasmid construction and preparation of gag-pro recombinant HIV-1 clones

Clinical HIV-1 isolates CL-1, CL-2, CL-3, and CL-4 were sequentially obtained from the same patient before and during NFV-containing treatment (Matsuoka-Aizawa et al., 2003). Direct sequences of these four clinical isolates and sub-cloning

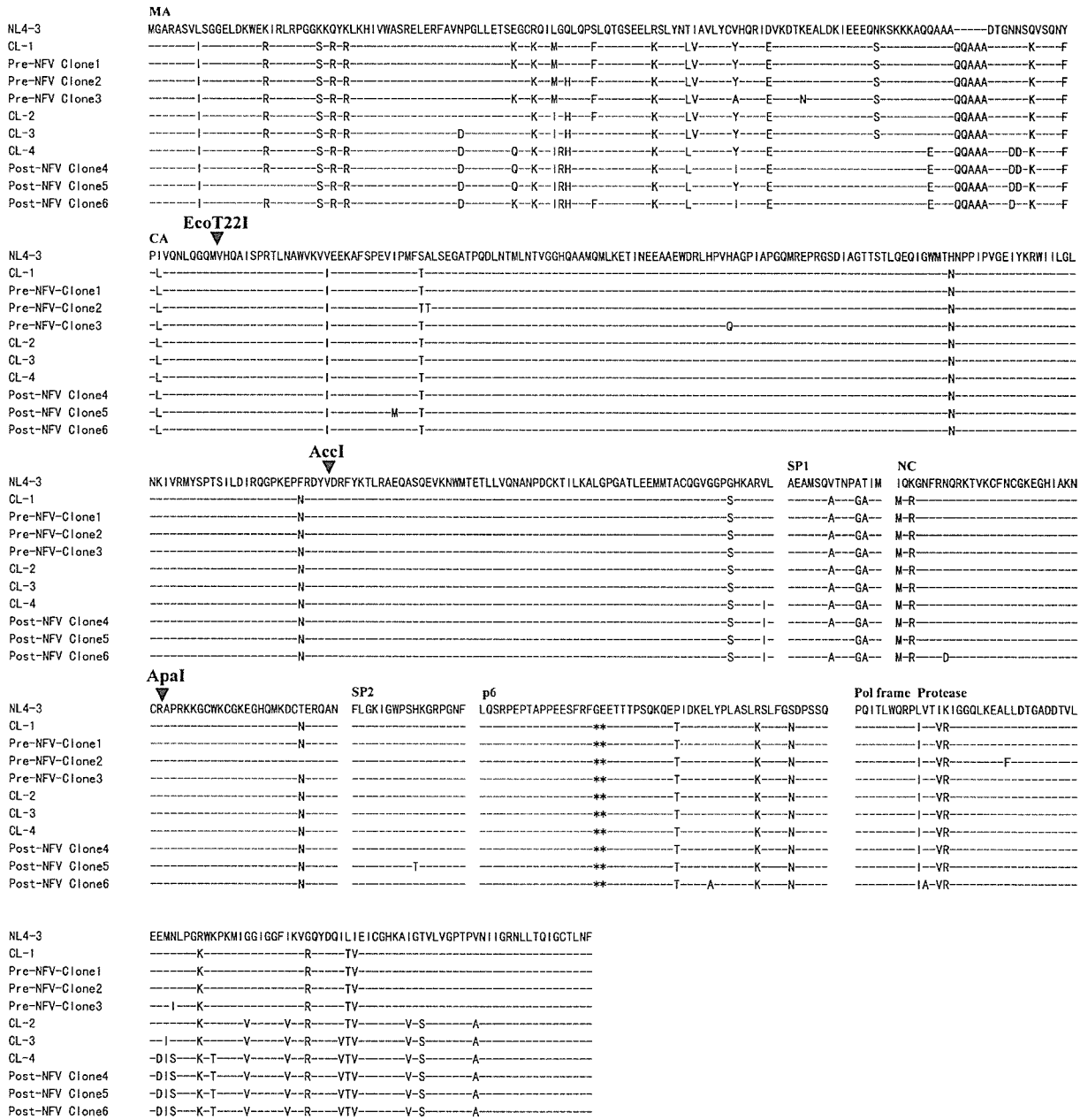

Fig. 1. Direct and sub-clonal sequences of clinical HIV-1 isolates. Direct and sub-clonal amino acid sequences of whole Gag and protease of HIV-1 isolates are shown. Pre-NFV Clone 1–3 and Post-NFV Clone 4–6 were derived from CL-1 and CL-4, respectively. The amino acid sequence of HIV-1_{NL4-3} is shown at the top as reference. The identical amino acids with those of HIV-1_{NL4-3} are indicated with dashes and the star shows deletion compared with HIV-1_{NL4-3} sequence. The restriction sites used in the construction of recombinant HIV-1 plasmids are also shown. MA, matrix; CA, Capsid; NC, nucleocapsid; and PR, protease.

sequences of CL-1 and CL-4 indicated that 11 and 10 amino acid substitutions accumulated in Gag and protease during PI-containing treatment, respectively (Fig. 1). Post-NFV Clone 4 (Fig. 1) was used in the construction of CL-4-derived recombinant HIV-1 plasmid. The pNL4-3-based plasmids of PRmt (HIV-1 carrying only the substitutions in protease of CL-4), p24PRmt (carrying the substitutions in capsid and protease of CL-4), and p17PRmt (carrying the substitutions in whole Gag and protease of CL-4) were constructed as previously described (Matsuoka-Aizawa et al., 2003) (Fig. 2), and the plasmids of MAmt (carrying only the substitutions in the matrix of CL-4) and MA + PRmt (carrying the substitutions in the matrix and protease of CL-4) were constructed by using the same restriction enzyme sites (Figs. 1 and 2). The plasmids of NCAmt (carrying the substitutions in matrix, N-terminal half of capsid, and protease of CL-4) and CCAmt (carrying the substitutions in matrix, C-terminal half of capsid, and protease of CL-4) were constructed by using AccI site. Originally, pNL4-3 has two AccI site between *gag* and protease region, one in the matrix, and the other in the capsid. However, since the one in the matrix was extinct due to natural substitution in CL-4, the other in the capsid was unique in *gag* and protease region.

HeLa cells (5×10^5 cells) were grown in DMEM with 10% FCS for 24 h and transfected with 3 μg of pNL4-3 and *gag*-protease recombinant HIV-1 plasmid DNAs by using FuGINE 6 transfection reagent (Roche Diagnosis, Basel, Switzerland). The cells were incubated for 24 h, washed once with PBS, and cultured in 5 ml of culture medium. The culture supernatant containing virus was collected at 48 h after transfection, filtered, analyzed for RT activity (10432–17162 cpm/μM), and kept at −80 °C until use. The virus titer used for infection and Western blot analysis was adjusted with RT activity.

2.3. HIV-1 replication kinetics

The methods used to infect cells were described previously (Matsuoka-Aizawa et al., 2003). Briefly, MT-2, PM-, and H9 cells (2×10^4) were infected with 200 μl of cell-free supernatant containing HIV-1 (2×10^5 ^{32}P cpm of RT activity) in the absence or presence of NFV (0.1 and 1 μM) for 16 h, washed once, and cultured in 200 μl of culture medium with the same concentration of NFV. A half volume of culture medium was changed every 2 or 3 days, and the supernatant was kept at −80 °C for measurement of RT activity. Each experiment was carried out in duplicate and repeated three times.

2.4. Competitive HIV-1 replication assay

H9 cells (2×10^5 cells) were incubated with two HIV-1 clones (each of 100 $TCID_{50}$) simultaneously for 16 h, washed with PBS twice, and cultured in the absence or presence of 0.1 μM NFV for 7 days. These infection periods were defined as a single passage. At the end of each passage, H9 cells were harvested and the culture supernatants were used to infect fresh

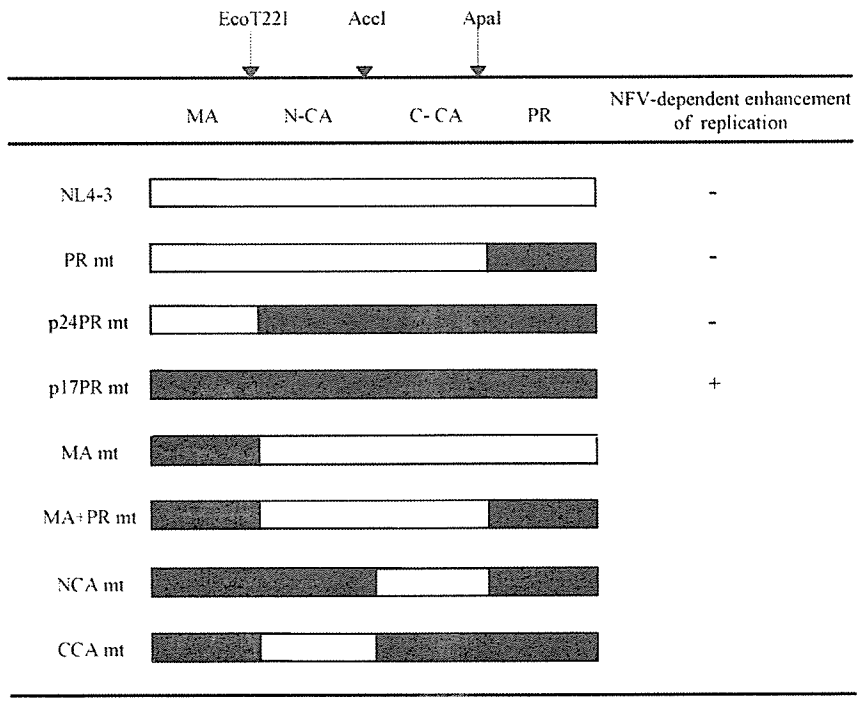

Fig. 2. Previously and newly constructed recombinant HIV-1s. The recombinant molecular clones were constructed based on pNL4-3 as a genetic backbone. The Gag-PR region of HIV-1 was segmented into four areas. MA (BssHII-EcoT22I fragment), N-terminal half of CA (NCA) (EcoT22I-AccI fragment), C-terminal half of CA (CCA) (AccI-ApaI fragment), and PR (ApaI-BalI fragment). Originally, pNL4-3 has two AccI sites between the gag and PR region, in MA and CA. However, because the one in MA was extinct in CL-4 due to natural substitution, the other AccI site in CA was unique for gag-PR gene of CL-4. Open boxes indicate the NL4-3-originated fragments, and closed boxes indicate fragments that were derived from CL-4 variants. The NFV-dependent replication enhancement of previously analyzed clones was also shown and indicated as (+). MA, matrix; CA, capsid; and PR, protease.

uninfected H9 cells. The cells harvested at each passage were subjected to PCR for amplification of HIV-1 *gag* region and direct DNA sequencing was performed. The viral populational changes were determined by relative peak height on sequence electrophoregram (Kosalaraksa et al., 1999).

2.5. HIV-1 susceptibility to NFV

MT-2 cells were infected with 500 $TCID_{50}$ of each virus in the absence and the presence of 0.001, 0.00316, 0.01, 0.0316, 0.1, 0.316, 1, and 3.16 μM of NFV, and cultured in triplicate for 7 days. At the end of culture, the amounts of p24 in the supernatants were measured and 50% inhibitory concentrations (IC_{50}) of NFV were determined by referring to the dose–response curve.

2.6. Western blot analysis of HIV-1 virions

HeLa cells were transfected with pNL4-3 and *gag*-protease recombinant HIV-1 plasmid DNA in the absence and presence of 0.1 μM NFV. The culture supernatant was harvested at 48 h after transfection, centrifuged at 37,000 × *g* for 90 min to pellet virus particles. The virion pellet (6×10^5 cpm of RT activity) was applied to an SDS gradient gel electrophoresis and transferred to a nitrocellulose membrane. The membrane was incubated with anti-HIV-1 p24 antisera (Advanced Biotechnology, Columbia, USA) and HIV-1-infected patients' serum, respectively, and hybridized with anti-protein A antibody conjugated with horseradish peroxidase (Amersham Pharmacia Biotech, Uppsala, Sweden). The immune complex was visualized with an ECL Plus system (Amersham Pharmacia Biotech) according to the manufactures' description.

The percent signal density of Gag products was analyzed on a Windows computer by using the ImageJ Program (developed at the U.S. National Institutes of Health ⟨http://www.rsb.info.nih.gov/ij/⟩) and the percent density of p24 was determined by the following formula: percent density of p24 = 100 × (the density of p24 signal)/(the cumulated density of all *Gag* signals) (Tamiya et al., 2004).

3. Results

3.1. Whole capsid substitutions necessary for NFV-enhanced replication

MAmt, carrying only the substitutions in the matrix (Fig. 2), grew well in the absence of NFV (Fig. 3). In the presence of NFV, however, it did not grow at all, indicating that matrix substitutions were not sufficient to confer NFV resistance. MA + PRmt, carrying substitutions in the matrix and protease (Fig. 2), replicated as efficiently as PRmt (carrying only the substitutions in protease), both in the absence and presence of 0.1 μM NFV, though its replication was not enhanced with NFV, indicating that the substitutions in matrix and protease were not sufficient for NFV-dependent enhancement of replication. As reported in our previous study (Matsuoka-Aizawa et al., 2003), p17PRmt replicated more efficiently in the presence of 0.1 μM NFV than in the absence of NFV. Therefore, some of the substitutions in the capsid should be responsible for such unique phenotype of CL-4 strain. The HIV-1 capsid contains two domains, a C-terminal oligomerization domain and N-terminal core domain, which function differently in viral assembly (Turner and Summers, 1999). Therefore, we divided the EcoT22I—ApaI segment of CL-4 into two segments at ACC I site, named them the N-terminal half of the capsid (NCA) and the C-terminal half of the capsid (CCA), and constructed two recombinant HIV-1 clones, NCAmt and CCAmt, which possessed all the substitutions in the matrix and protease of CL-4, and the substitutions in NCA and CCA, respectively (Fig. 2). NCAmt and CCAmt grew efficiently both in the absence and presence of 0.1 μM NFV, and only NCAmt showed weak replication enhancement with 0.1 μM NFV in PM-1 and MT-2 cells though it was not so efficient as that of p17PRmt, suggesting that the substitutions in CCA, contributed to the efficient replication enhancement of p17PRmt (Fig. 3). CCAmt did not show the p17PRmt's phenotype, indicating that the substitutions in NCA were indispensable for replication enhancement. As we reported previously (Matsuoka-Aizawa et al., 2003), p24PRmt lacking the substitutions in matrix did not show replication enhancement by NFV. Taken together, the substitutions in the whole matrix, capsid, SP1, and the N-terminal end of nucleocapsid of CL-4 were indispensable for efficient replication enhancement of p17PRmt.

To define further the role of substitutions in the matrix, NCA, and CCA, viral replication efficiency was compared among the HIV-1 clones described above in the absence and presence of NFV using competitive HIV-1 replication assay (Kosalaraksa et al., 1999). MA + PRmt outgrew PRmt both in the absence and presence of 0.1 μM NFV (Fig. 4a), and MAmt was outgrown by NL4-3 in the absence of NFV (Fig. 4b), suggesting that the substitutions in the matrix of CL-4 reduced the replication of HIV-1 harboring wild-type protease, but compensated the replication of HIV-1 harboring NFV-resistant protease of CL-4. NCAmt outgrew MA + PRmt both in the absence and presence of 0.1 μM NFV (Fig. 4c), suggesting that the substitutions in NCA were compensatory for the replication of HIV-1 harboring protease and matrix of CL-4. However, CCAmt was outgrown by MA + PRmt in the absence of NFV, but its replication in the presence of 0.1 μM NFV was comparable with that of MA + PRmt under similar condition (Fig. 4d), suggesting that the substitutions in CCA reduced the replication capability of MA + PRmt, while NFV compensated the mutation effect. Sub-cloning analyses of proviral sequences at both of the passages 3 and 4 in competitive HIV-1 replication assay in the presence of 0.1 μM NFV showed that five of 10 clones were derived from CCAmt and the other five clones were derived from MA + PRmt, which confirmed that CCAmt and MA + PRmt had comparable replication ability in the presence of 0.1 μM NFV (Fig. 4d). MA + PRmt readily outgrew p17PRmt in the absence of NFV, but was outgrown by p17PR in the presence of 0.1 μM NFV (Fig. 4e), suggesting that the substitutions in NCA and CCA reduced the replication capability of MA + PRmt, while NFV counteracted the mutation effect and rather enhanced replication ability at sub-inhibitory concentration (Fig. 3, p17PRmt).

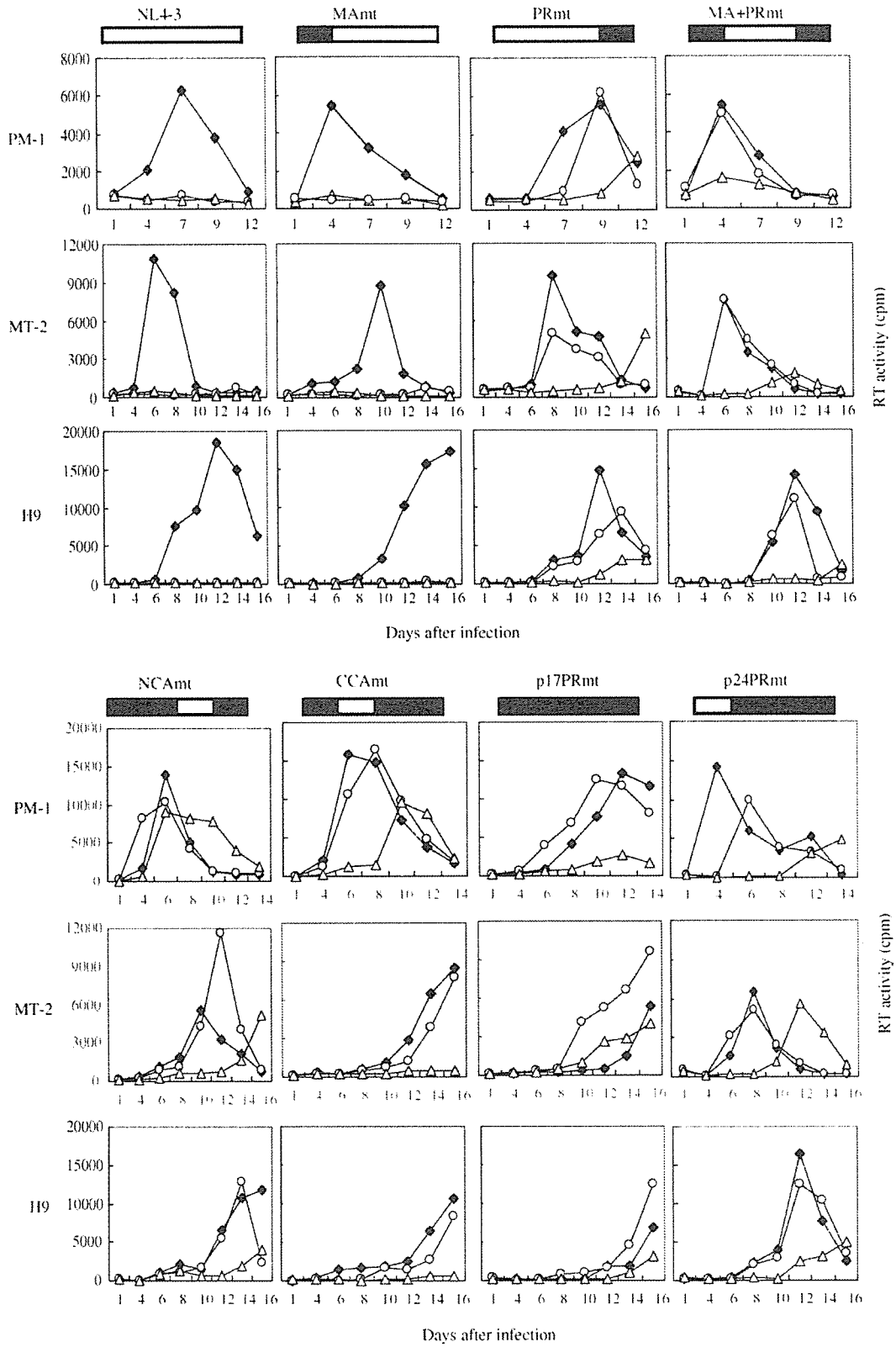

Fig. 3. Effects of NFV on replication capability of recombinant HIV-1s. PM-1, MT-2, and H9 cells (2×10^4 cells) were exposed to 0.2 ml of cell-free supernatant containing each HIV-1 clone (2×10^5 ^{32}P cpm of RT activity), washed once, and cultured in 0.2 ml of medium in the absence (closed diamonds) and presence of NFV (0.1 μM; open circles, 1 μM; open triangles). Half volume of the culture medium was changed every 2 or 3 days, and the supernatant was kept at −80 C until the measurement of RT activity. Each experiment was carried out in duplicate and repeated three times, and representative data are shown.

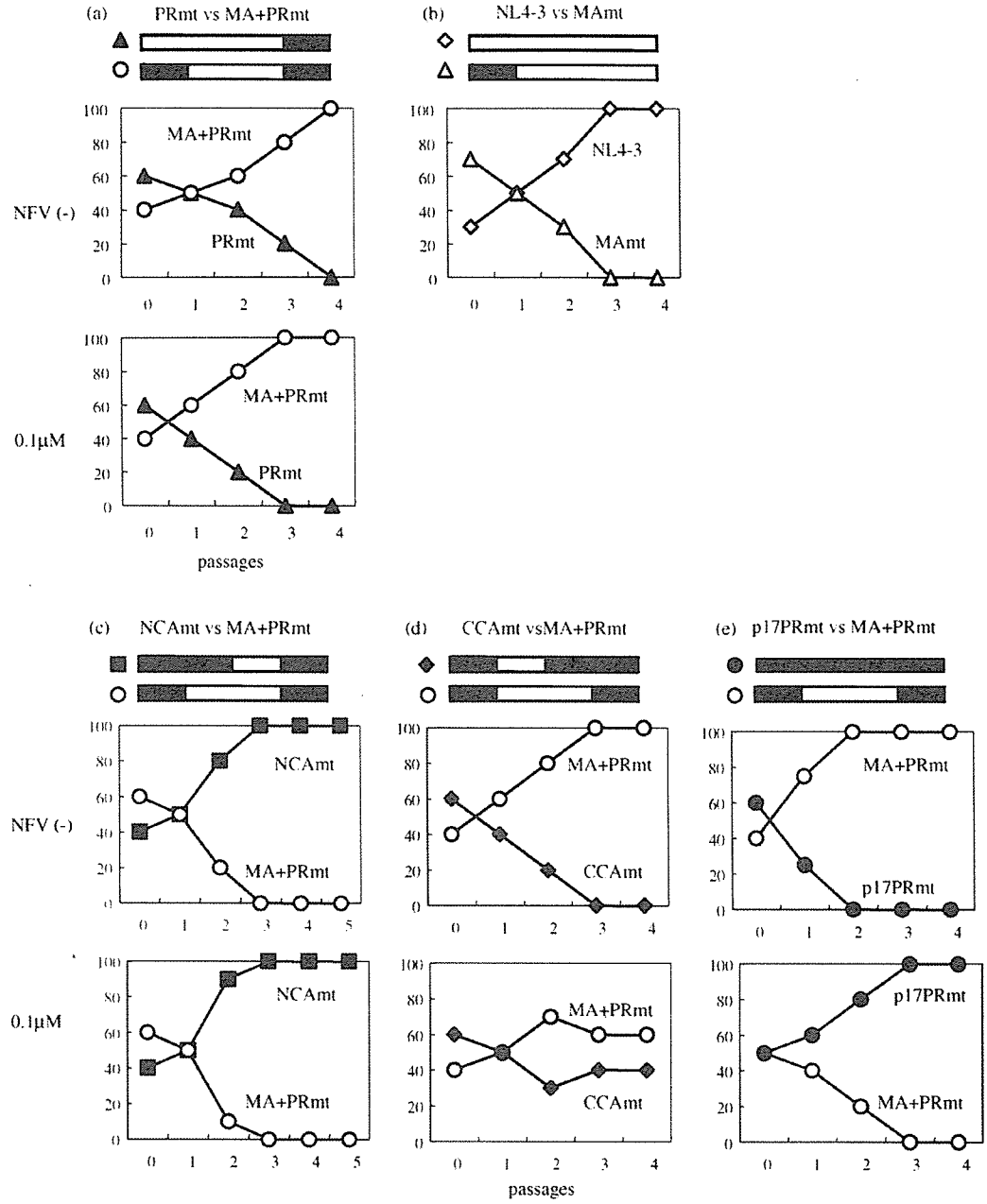

Fig. 4. One-to-one competitive HIV-1 replication assay. H9 cells (2×10^5 cells) were incubated with two recombinant HIV-1s (each of 100 $TCID_{50}$) simultaneously at 37 C for 16 h, washed with PBS twice, and cultured in the absence and presence of 0.1 μM of NFV. At 7 days post-infection, the culture supernatant was used to infect fresh uninfected H9 cells. The cells harvested at each passage were subjected to direct DNA sequencing, and the viral population changes were determined by the relative peak height in the sequencing electrophoregram. The persistence of the original amino acid substitutions was confirmed for all infectious clones used in this assay. (a) PRmt vs. MA + PRmt; (b) NL4-3 vs. MAmt; (c) NCAmt vs. MA + PRmt; (d) CCAmt vs. MA + PRmt; (e) p17PRmt vs. MA + PRmt.

3.2. Gag substitutions conferring NFV resistance

To analyze the role of the substitutions in the matrix, NCA, and CCA in NFV resistance, IC_{50}s of NFV for the HIV-1 clones described above were determined by using MT-2 cells (Zhang et al., 1997). MAmt (IC_{50}: 9.4 nM) showed 1.9-fold resistance against NFV compared with NL4-3 (5.0 nM), and p17PRmt (893 nM) showed 3.3-fold resistance compared with p24PRmt (273 nM) (Table 1), indicating that the substitutions in the matrix may make a small contribution to the viral resistance against NFV. NCAmt (483 nM) had 2.1-fold resistance against NFV compared with MA + PRmt (229 nM), and p17PRmt had 4.1-fold resistance compared with CCAmt (217 nM), indicating that the substitutions in NCA gave positive impact on viral resistance. Interestingly, CCAmt showed 0.95-fold resistance against NFV compared with MA + PRmt, indicating that substitutions in CCA

Table 1
NFV resistance of recombinant HIV-1s

HIV-1	IC_{50} (nM)	Fold-resistance
NL4-3	5.0 ± 0.4	1.0
PRmt	241 ± 34	4.8
p24PRmt	273 ± 13	5.5
p17PRmt	893 ± 28	18
MAmt	9.4 ± 3.3	1.9
MA + PRmt	229 ± 21	46
NCAmt	483 ± 26	97
CCAmt	217 ± 32	43

The concentrations of drug added to the growth medium for calculation of the IC_{50}s were 0, 1, 3.16, 10, 31.6, 100, and 316 nM and 1 and 3.16 μM NFV, and the IC_{50}s were derived from plots of percent of inhibition of p24 production in culture supernatant versus NFV concentration.

may give small negative impact on viral resistance in the absence of the substitutions in NCA. p17PRmt, however, had 1.8-fold resistance compared with NCAmt, indicating the substitutions in CCA may give a small but positive contribution to viral resistance in the presence of the substitutions in NCA. The role of the substitutions in CCA in viral resistance was altered by the presence of the substitutions in NCA.

3.3. *Gag substitutions facilitating cleavage between matrix and capsid*

To further delineate the impact of each substitution, the Gag processing pattern was assessed in the absence and presence of NFV by Western blot analysis using anti-p24 monoclonal antibody (Fig. 5A1–2 and B1–2). As expected, 0.1 μM of NFV effectively blocked cleavage of the Gag p55 precursor of NL4-3 (percent density of p24; 4.7% versus 87.5% in Fig. 5A1; 4.2% versus 83.3% in Fig. 5A2). In contrast, NFV gave only a small influence on the cleavage patterns of the p55 precursor of MA + PRmt (percent density of p24; 65.5% versus 87.4% in Fig. 5A1; 77.8% versus 92.6% in Fig. 5A2), which is consistent with the indistinguishable replication kinetics of this mutant in the absence and presence of NFV (Fig. 3). Interestingly, NFV enhanced the cleavability of the p55 precursor of p17PRmt (percent density of p24; 94.8% versus 74.3% in Fig. 5A1; 72.2% versus 54.1% in Fig. 5A2), which was paralleled with NFV-dependent replication enhancement of this mutant (Fig. 3). NFV also gave a small positive effect on the cleavability of the p55 precursor of NCAmt (percent density of p24; 97.1% versus 94.6% in Fig. 5B1; 97.5% versus 96.2% in Fig. 5B2), which was paralleled with the partial enhancement of replication with NFV (Fig. 3). Furthermore, percent density of p24 of NCAmt was increased compared with that of MA + PRmt (percent density of p24; 94.6% and 96.2% versus 87.4% and 92.6% in the absence of NFV; 97.1% and 97.5% versus 65.5% and 77.8% in the presence of 0.1 μM NFV), suggesting that the substitutions in NCA play a significant role in Gag cleavability. Finally, NFV decreased percent density of p24 of CCAmt (percent density of p24; 68.9% versus 78.2% in Fig. 5B1; 45.3% versus 79.0% in Fig. 5B2), which was paralleled with NFV-induced delay of replication kinetics (Fig. 3). For further confirmation, the Gag processing pattern of NCAmt and CCAmt was also assessed by Western blot analysis using HIV-1-infected patient's serum (Fig. 5B3). As expected, NFV slightly increased cleavability of the p55 precursor of NCAmt (percent density of p24; 96.9% versus 94.5% in Fig. 5B3), and gave a negative impact on Gag cleavage of CCAmt (percent density of p24; 41.9% versus 74.3% in Fig. 5B3), which were well compatible with the cleavage pattern analyzed by using anti-p24 monoclonal antibody (Fig. 5B1, 2). In summary, NFV induced enhanced cleavability of Gag precursors of p17PRmt and NCAmt, which was well paralleled with NFV-induced enhancement of replication capability of these mutants.

4. Discussion

We previously reported that the substitutions in p6-protease segment alone are sufficient to confer NFV resistance while those in matrix are indispensable for the replication enhancement of CL-4 by NFV (Matsuoka-Aizawa et al., 2003). In the present study, we found that not only the matrix substitutions but the mutations in N-terminal half of capsid also played critical role in the enhancement and that the full potential of the enhancement phenotype was achieved only with the cooperation of mutations in the entire Gag and protease region of CL-4. The substitutions in matrix and those in N-terminal half of capsid compensated the otherwise compromised viral replication in the absence and presence of NFV (Fig. 4a and c). Probably, these substitutions cooperatively altered the tertiary structure of the Gag precursor and made the cleavage site between matrix and capsid more accessible to mutant protease harboring multiple resistance-associated mutations. The cleavage pattern analyzed by Western blot analysis supported the idea that the substitutions in N-terminal half of capsid improved the Gag cleavage. Percent density of p24 of NCAmt was increased compared with that of MA + PRmt in the absence of NFV (Fig. 5A1–2 and B1–2; 94.6% and 96.2% versus 87.4% and 92.6%). It is worth noting that CL-4 had a total of 56 amino acid substitutions in *gag-pro* genes compared with NL4-3; 22 substitutions had emerged during NFV-containing therapy, and 34 other substitutions had already existed before the introduction of the therapy, and that all the substitutions in N-terminal half of capsid of CL-4 were pre-existing before NFV-therapy (Fig. 1), suggesting that certain polymorphic amino acid residues seen in HIV-1 clinical isolates were associated with drug resistance. Interestingly, the amino acid insertion at the same site of the matrix of CL-4 compared with NL4-3 (Fig. 1; amino acids 121–125 in MA, QQAAA) was reported to increase viral replication harboring mutant protease by improving otherwise impaired Gag processing (Tamiya et al., 2004). Gatanaga et al. also reported that a polymorphic substitution in N-terminal half of capsid was indispensable for the development of high multitude of resistance against PIs (Gatanaga et al., 2002), though CL-4 did not harbor the same substitution. It is also known that certain drug-resistance-conferring amino acid substitutions found in one subtype HIV-1 isolated from patients under therapy may be detected in HIV-1 of other subtypes from untreated individuals (Cornelissen et al., 1997; Quinones-Mateu et al., 1998). More-

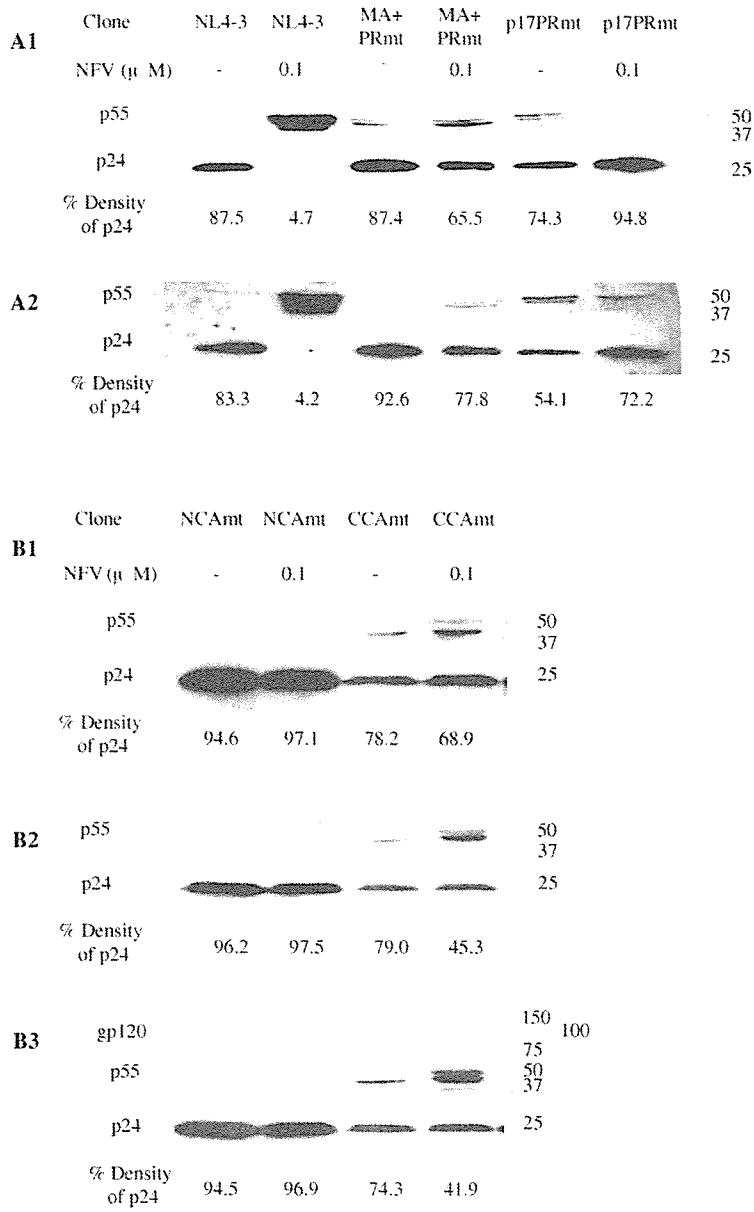

Fig. 5. Western blot analysis in the absence and presence of NFV. HeLa cells were transfected with each of full-length molecular clones and cultured in the absence and presence of 0.1 μM NFV. At 48 h post-transfection, virions in the culture supernatant (6×10^5 cpm of RT activity) were harvested and subjected to Western blot analysis. Gag proteins were visualized by using anti-p24 monoclonal antibody (A1-2, B1-2) and HIV-1-infected patient's serum (B3). Percent density of p24 was calculated as 100 × (p24 signal density/total Gag product signal densities) in a Western blot.

over, a recent study of Colson et al. revealed that HIV-2 strains harbor specific patterns of natural polymorphism and resistance (Colson et al., 2004). HIVs seem to acquire drug-resistance by utilizing the pre-existing polymorphic mutations and by coordinating the development of multiple substitutions.

Furthermore, the substitutions in N-terminal half of capsid of CL-4 altered the effect of NFV on viral replication. Sub-inhibitory concentration (0.1 μM) of NFV slightly accelerated the Gag precursor cleavage of NCAmt (percent density of p24; 97.1% versus 94.6% in Fig. 5B1; 97.5% versus 96.2% in Fig. 5B2; 96.9% versus 94.5% in Fig. 5B3), which was paralleled with the partial replication enhancement with NFV (Fig. 3), though it showed inhibitory effect in Gag processing of MA + PRmt (percent density of p24; 65.5% versus 87.4% in Fig. 5A1; 77.8% versus 92.6% in Fig. 5A2). Therefore, one of the mechanisms of viral replication enhancement with NFV is the improved processing of Gag harboring the substitutions in N-terminal half of capsid of CL-4 cooperated with the substitutions in the matrix. On the other hand, the role of the substitutions in C-terminal half of capsid seemed different, though they were also indispensable for the full potential of replication enhancement with NFV. They impaired the cleavability of Gag precursor

of MA + PRmt (Fig. 5A1–2 and B1–2; percent density of p24; CCAmt versus MA + PRmt = 78.2% and 79.0% versus 87.4% and 92.6%) and NCAmt (Fig. 5A1–2 and B1–2; percent density of p24; p17PRmt versus NCAmt = 74.3% and 54.1% versus 94.6% and 96.2%) in the absence of NFV, which were parallel with viral replication data (CCAmt versus MA + PRmt, Fig. 4d; p17PRmt versus NCAmt, Fig. 3). The effects of NFV on Gag cleavage pattern were different between CCAmt and p17PRmt; sub-inhibitory concentration (0.1 μM) of NFV facilitated the Gag cleavability of p17PRmt (percent density of p24; 94.8% versus 74.3% in Fig. 5A1; 72.2% versus 54.1% in Fig. 5A2), though it decreased the cleavability of CCAmt Gag (percent density of p24; 68.9% versus 78.2% in Fig. 5B1; 45.3% versus 79.0% in Fig. 5B2; 41.9% versus 74.3% in Fig. 5B3), which was also parallel with viral replication data showing enhancement only in p17PRmt but not in CCAmt (Fig. 3). Considering together, the substitutions in C-terminal half of capsid compromised viral replication by impairing the Gag preprocessing, and NFV could counteract the negative impact only in the presence of the substitutions in N-terminal half of capsid. In the absence of the substitutions in N-terminal half of capsid, only partial counteraction was seen (Fig. 4d). In summary, NFV-induced viral replication enhancement of CL-4 was caused by two mechanisms; NFV facilitates the processing of Gag harboring the substitutions in the matrix and N-terminal half of capsid of CL-4, and NFV counteracts the impaired Gag cleavage caused by the substitutions in C-terminal half of capsid of CL-4 only in the presence of the substitutions in the matrix and N-terminal half of capsid of CL-4. Therefore, the full potential of the enhancement phenotype was achieved only with the cooperation of mutations in the entire Gag and protease region of CL-4.

Notably, we found several other PI-resistant isolates with the phenotype of PI-dependent replication enhancement (data not shown), suggesting that HIV-1 can evolve to acquire capability to replicate better with the drugs. Such replication enhancement with antiretroviral agents presents formidable challenge in the therapy of HIV-1 infection. Future studies of structural analyses of Gag precursor(s) harboring substitutions of these mutants are warranted to clarify the underlying mechanism(s).

Acknowledgments

The authors thank A. Hachiya, K. Tsuchiya, Y. Suzuki, and Y. Hirabayashi for their helpful suggestions and continuous discussions throughout this study. We are also indebted to Y. Takahashi and F. Negishi for their technical assistance. This study was supported by a Grant-in-Aid for AIDS Research from the Ministry of Health, Labor, and Welfare of Japan (H15-AIDS-001), by the Organization of Pharmaceutical Safety and Research (01-4), and by the Japanese Foundation for AIDS Prevention.

References

Bleiber, G., Munoz, M., Ciuffi, A., Meylan, P., Telenti, A., 2001. Individual contributions of mutant protease and reverse transcriptase to viral infectivity, replication, and protein maturation of antiretroviral drug-resistant human immunodeficiency virus type 1. J. Virol. 75, 3291–3300.

Colson, P., Henry, M., Tourres, C., Lozachmeur, D., Gallais, H., Gastaut, J.A., Moreau, J., Tamalet, C., 2004. Polymorphism and drug-selected mutations in the protease gene of human immunodeficiency virus type 2 from patients living in southern France. J. Clin. Microbiol. 42, 570–577.

Cornelissen, M., van den Burg, R., Zorgdrager, F., Lukashov, V., Goudsmit, J., 1997. pol gene diversity of five human immunodeficiency virus type 1 subtypes: evidence for naturally occurring mutations that contribute to drug resistance, limited recombination patterns, and common ancestry for subtypes B and D. J. Virol. 71, 6348–6358.

Croteau, G., Doyon, L., Thibeault, D., McKerche, G., Pilote, L., Lamarre, D., 1997. Impaired fitness of human immunodeficiency virus type 1 variants with high-level resistance to protease inhibitors. J. Virol. 71, 1089–1096.

Doyon, L., Croteau, G., Thibeault, D., Poulin, F., Pilote, L., Lamarre, D., 1996. Second locus involved in human immunodeficiency virus type 1 resistance to protease inhibitors. J. Virol. 70, 3763–3769.

Gatanaga, H., Suzuki, Y., Tsang, H., Yoshimura, K., Kavlick, M.F., Nagashima, K., Gorelick, R.J., Mardy, S., Tang, C., Summers, M.F., Mitsuya, H., 2002. Amino acid substitutions in Gag protein at non-cleavage sites are indispensable for the development of a high multitude of HIV-1 resistance against protease inhibitors. J. Biol. Chem. 277, 5952–5961.

Kosalaraksa, P., Kavlick, M.F., Maroun, V., Le, R., Mitsuya, H., 1999. Comparative fitness of multi-dideoxynucleoside-resistant human immunodeficiency virus type 1 (HIV-1) in an *in vitro* competitive HIV-1 replication assay. J. Virol. 73, 5356–5363.

Martinez-Picado, J., Savara, A.V., Sutton, L., D'Aquila, R.T., 1999. Replicative fitness of protease inhibitor-resistant mutants of human immunodeficiency virus type 1. J. Virol. 73, 3744–3752.

Matsuoka-Aizawa, S., Sato, H., Hachiya, A., Tsuchiya, K., Takebe, Y., Gatanaga, H., Kimura, S., Oka, S., 2003. Isolation and molecular characterization of a nelfinavir (NFV)-resistant human immunodeficiency virus type 1 that exhibits NFV-dependent enhancement of replication. J. Virol. 77, 318–327.

Quinones-Mateu, M.E., Albright, J.L., Mas, A., Soriano, V., Arts, E.J., 1998. Analysis of pol gene heterogeneity. Viral quasispecies, and drug resistance in individuals infected with group O strains of human immunodeficiency virus type 1. J. Virol. 72, 9002–9015.

Tamiya, S., Mardy, S., Kavlick, M.F., Yoshimura, K., Mistuya, H., 2004. Amino acid insertions near Gag cleavage sites restore the otherwise compromised replication of human immunodeficiency virus type 1 variants resistant to protease inhibitors. J. Virol. 78, 12030–12040.

Turner, B.G., Summers, M.F., 1999. Structural biology of HIV. J. Mol. Biol. 285, 1–32.

Zhang, Y.M., Imamichi, H., Imamichi, T., Lane, H.C., Falloon, J., Vasudevachari, M.B., Salzman, N.P., 1997. Drug resistance during indinavir therapy is caused by mutations in the protease gene and in its Gag substrate cleavage sites. J. Virol. 71, 6662–6670.

Journal of Antimicrobial Chemotherapy Advance Access published July 26, 2006

Journal of Antimicrobial Chemotherapy
doi:10.1093/jac/dkl297

JAC

Role of type II topoisomerase mutations and AcrAB efflux pump in fluoroquinolone-resistant clinical isolates of *Proteus mirabilis*

Ryoichi Saito[1,2]*, Kenya Sato[2], Wakako Kumita[2], Natsuko Inami[2], Hiroyuki Nishiyama[2], Noboru Okamura[2], Kyoji Moriya[1] and Kazuhiko Koike[1]

[1]*Department of Infection Control and Prevention, The University of Tokyo Hospital, Bunkyo-ku, Tokyo 113-8655, Japan;* [2]*Department of Microbiology and Immunology, Graduate School of Allied Health Sciences, Tokyo Medical and Dental University, Bunkyo-ku, Tokyo 113-8510, Japan*

Received 10 March 2006; returned 7 April 2006; revised 28 June 2006; accepted 2 July 2006

***Objectives*: We conducted a study to determine the role played by amino acid mutations in DNA gyrase and topoisomerase IV, and the AcrAB efflux pump in resistance to fluoroquinolones in clinical isolates of *Proteus mirabilis*.**

***Methods*: Nine clinical isolates of *P. mirabilis* containing eight fluoroquinolone-resistant isolates and one fluoroquinolone-susceptible isolate as the causative pathogen were collected from different patients with urinary tract infections. Fluoroquinolone resistance was characterized by PCR and DNA sequencing. The role of the AcrAB efflux pump was investigated by semi-quantifying the transcriptional expression of the *acrB* gene.**

***Results*: Double mutations were found in GyrA, at S83I and E87K, and single mutations in GyrB (S464F) and ParC (S80I) in four isolates with ciprofloxacin MICs of 16 to >128 mg/L. In three isolates (ciprofloxacin MICs of >128 mg/L), the level of *acrB* expression was 2.1- to 3.2-fold higher than that in the wild-type control strain (ciprofloxacin MIC of ≤0.12 mg/L) and these isolates also had increased MICs of minocycline (>64 versus 8–16 mg/L) and chloramphenicol (>256 versus 4–8 mg/L) compared with the five other fluoroquinolone-resistant isolates.**

***Conclusion*: Our findings demonstrate that two mechanisms—mutations in GyrA (at S83I and E87K), GyrB and ParC, and overproduction of the AcrAB efflux pump—might synergistically contribute to a highest level of resistance to fluoroquinolones in clinical isolates of *P. mirabilis*.**

Keywords: *P. mirabilis*, DNA gyrase, topoisomerase IV

Introduction

Among Enterobacteriaceae, *Proteus mirabilis* is one of the most common causes of urinary tract infections (UTIs), which are often persistent and difficult to treat, and is also an important cause of nosocomial infections.[1] Though wild-type strains of *P. mirabilis* are usually susceptible to fluoroquinolones, a progressive increase in fluoroquinolone resistance has been seen in clinical isolates of the bacterium.[2,3]

Two mechanisms that decrease susceptibility to fluoroquinolones have been identified so far in clinical isolates, which are alteration of the target proteins—DNA gyrase (encoded by *gyrA* and *gyrB* genes) and topoisomerase IV (encoded by *parC* and *parE* genes)—and reduced drug accumulation due to efflux pumps.[4] In *P. mirabilis*, development of fluoroquinolone resistance requires a combination of two or more mutations in the quinolone resistance-determining region (QRDR) of the genes encoding DNA gyrase and topoisomerase IV and is mainly attributed to amino acid mutations at positions Ser-83 in GyrA, Ser-464 in GyrB and Ser-80 in ParC.[5] In addition, there is growing evidence for the implication of the overexpression of multidrug efflux pumps in fluoroquinolone resistance in other bacteria, such as AcrAB in *Escherichia coli*[6,7] and *Salmonella enterica* serovar Typhimurium[8,9] or CmeABC in *Campylobacter* species.[10] Moreover, the AcrAB efflux pump has been determined to be associated with reduced levels of susceptibility to tigecycline and minocycline in *P. mirabilis*[11] but the role of this efflux pump in the fluoroquinolone resistance of *P. mirabilis* has been unclear.

*Corresponding author. Department of Infection Control and Prevention, The University of Tokyo Hospital, 7-3-1 Hongo, Bunkyo-ku, Tokyo 113-8655, Japan. Tel: +81-3-3815-5411; Fax: +81-3-5689-0495; E-mail: saito-lab@h.u-tokyo.ac.jp

Much data need to be collected from clinical isolates to assess risks from the increasing fluoroquinolone resistance of *P. mirabilis*. We therefore investigated the roles played by amino acid mutations in DNA gyrase and topoisomerase IV and the AcrAB efflux pump in the fluoroquinolone resistance of clinical isolates of *P. mirabilis*.

Materials and methods

Bacterial strains and susceptibility testing

The bacterial strains used in this study were those of *P. mirabilis* present in nine clinical isolates from different patients with acute, repeated or chronic UTIs at the University of Tokyo Hospital, collected from October 2003 through September 2005. All strains were identified by the conventional method and by the Vitek I system (bioMerieux Japan, Tokyo, Japan). Fluoroquinolones (ciprofloxacin, levofloxacin and sparfloxacin), minocycline, ampicillin, ceftazidime, gentamicin and imipenem were tested using panels manufactured by Eiken Chemical (Tokyo, Japan). Chloramphenicol (Sankyo, Tokyo, Japan), erythromycin (Shionogi Pharmaceutical, Osaka, Japan) and clarithromycin (Taishotoyama Pharmaceutical, Tokyo, Japan) were also used in this study. The MICs were determined by the broth microdilution method as described by the Clinical and Laboratory Standards Institute [CLSI, formerly known as the National Committee for Clinical Laboratory Standards (NCCLS)].[12] Quality control for the MICs was performed using the following reference strains: *Staphylococcus aureus* ATCC 21293, *E. coli* ATCC 25922 and *Pseudomonas aeruginosa* ATCC 27853.

PFGE

Genomic DNA of the *P. mirabilis* strains was prepared in agarose plugs that had been treated with lysozyme and pronase K using a Gene Path reagent kit (Bio-Rad, Tokyo, Japan) according to the manufacturer's recommendations. DNA was digested with 25 U of the restriction endonuclease *Not*I (Roch Diagnostics, Tokyo, Japan). The DNA fragments generated were then separated in a 1% agarose gel and subjected to electrophoresis in Tris–borate–EDTA buffer at 14°C using a pulsed-field apparatus (CHEF-DR II, Bio-Rad) at 200 V for 19.7 h with pulse times of 5–35 s. BioNumerics software (version 3.0; Applied Maths, Kortrijk, Belgium) was used to analyse the DNA restriction patterns and determine their similarity, based on calculation of the Dice similarity coefficient and using the UPGMA algorithm (unweighted pair-group method using arithmetic averages).

PCR amplification and sequencing of QRDRs of gyrA, gyrB and parC genes

The DNA template for PCR amplification was obtained from the supernatant of a boiled extract of *P. mirabilis* cells harvested from Luria–Bertani (LB) broth. The QRDRs of the *gyrA*, *gyrB* and *parC* genes were amplified using primer sets according to a method described previously.[5] PCR products were purified using the QIAquick PCR Purification Kit (Qiagen, Tokyo, Japan) in accordance with the manufacturer's recommendations. Purified PCR fragments were sequenced with an ABI PRISM 310 DNA sequencer (Applied Biosystems, Foster City, CA, USA). A similarity search for the deduced amino acid sequences against DDBJ/EMBL/GenBank sequence databases with the accession numbers AF397169 (*gyrA*), AF503506 (*gyrB*) and AF363611 (*parC*) from *P. mirabilis* ATCC 29906 was conducted using the BLAST program at the DNA Databank of Japan (Shizuoka, Japan).

Analysis of acrB gene expression by reverse transcription (RT)–PCR

Semi-quantitative RT–PCR was used to analyse the transcriptional expression of the *acrB* gene indicating expression of the AcrAB efflux pump. Overnight bacteria cultures were diluted 1:100 in LB broth and grown to the mid-logarithmic phase (OD_{600} = 0.5) at 37°C with shaking. Cultures were pelleted by centrifugation at 13 000 **g** for 10 min, and RNA was isolated using ISOGEN (Nippongen, Tokyo, Japan) according to the manufacturer's instructions. Total RNA (1 μg), 50 ng of random hexamers and 2 μL of a 10 mM deoxynucleoside triphosphates mixture (Invitrogen, Tokyo, Japan) were incubated for 5 min at 65°C, immediately cooled on ice and then reverse transcribed in a final volume of 20 μL—containing 2 μL of 10 mM dithiothreitol, 40 U of RNaseOUT ribonuclease inhibitor, First Strand Buffer 1× and 50 U of Superscript II reverse transcriptase (Invitrogen)—that was reacted for 50 min at 50°C. PCR amplification of cDNA was performed with an initial denaturation step of 5 min at 95°C, followed by 16 cycles of 30 s at 95°C, 30 s at 55°C and 1 min at 72°C, and finishing with one cycle of 7 min at 72°C, using primer sets for the *acrB* gene (Table 1). The number of PCR cycles used came within the linearity range for PCR amplification and constitutive expression of 16S rRNA assessed from the same cDNA preparation was used as a standard. Samples (10 μL) of each PCR product were separated by electrophoresis in 2.0% agarose and visualized by ethidium bromide staining. The bands of the *acrB* gene were semi-quantified using image scanning software (Scion Image) and results were standardized with the 16S rRNA band density.

Statistics

The above gene expression experiment was repeated three times. Results were expressed as mean±SD. Statistical analysis was performed with a two-tailed Student's *t*-test. P values <0.05 were taken as significant.

Nucleotide sequence accession number

The partial DNA sequences of the *gyrA* gene in isolates PmNC and Pm506 have been assigned to the DDBJ/EMBL/GenBank database

Table 1. Primers used in the study

Target gene	Primer name	Oligonucleotide sequence (5′–3′)	Annealing temp. (°C)	Product size (bp)[a]	GenBank accession no.
acrB	acrB-F	CGTCTATCAGGTAACCAAGC	55	298	AY061647
	acrB-R	TAACGTCGCTTCTACTAGCC			
16S rRNA	16S-F	GAGTTTGATCATGGCTCAG	55	322	U00096
	16S-R	CCCACTGCTGCCTCCCGT			

[a]Size of RT–PCR products.

under accession numbers AB252193 (PmNC) and AB252194 (Pm506).

Results

PFGE

The genetic similarity of the nine isolates was evaluated using PFGE. Eight PFGE types were identified and among them isolates Pm506 and Pm609 were identical being of type E. Table 2 summarizes the results.

Mutations in gyrA, gyrB and parC genes

The nucleotide sequences and derived amino acid sequences in the QRDRs of the *gyrA, gyrB* and *parC* genes for each *P. mirabilis* isolate were compared with those of the wild-type strain, ATCC 29906 (Table 2). One strain (PmNC) with a ciprofloxacin MIC of ≤0.12 mg/L showed no changes in GyrA, GyrB and ParC. Four isolates (Pm210, Pm405, Pm701 and Pm909) with ciprofloxacin MICs of 4–16 mg/L had a single mutation of Ser-83 to Arg or Ile in GyrA. Double mutations in GyrA, at Ser-83 and Glu-87, were found in four isolates (Pm311, Pm506, Pm609 and Pm805) having ciprofloxacin MICs of 16 to >128 mg/L. In these strains, the AGT codon for Ser-83 and the GAA codon for Glu-87 in the *gyrA* gene were replaced by ATT for Ile and AAA for Lys, respectively (Table 2). Further, all isolates showing resistance to ciprofloxacin (MIC of ≥4 mg/L) had one silent nucleotide substitution, a C to T transition for nucleotide position 148 of the *gyrA* gene, as compared with the *P. mirabilis* type strain, ATCC 29906. For GyrB, mutations such as Ser-464 to Tyr or Phe were detected in ciprofloxacin-resistant isolates (MICs of ≥8 mg/L), while no amino acid changes were detected at position 466 (Table 2). Furthermore, four isolates (Pm311, Pm506, Pm609 and Pm805) with a mutation of Ser-464 to Phe in GyrB showed a high level of resistance to ciprofloxacin (MICs of 16 to >128 mg/L). Except the isolate with a ciprofloxacin MIC of ≤0.12 mg/L, all isolates had amino acid changes affecting ParC: six isolates with Ser-80 to Ile and two isolates with Ser-80 to Arg (Table 2). No amino acid changes were detected at position 78 in ParC.

Expression of acrB gene

To determine the resistance to fluoroquinolones due to the AcrAB efflux pump, transcriptional expression of the *acrB* gene in the clinical isolates of *P. mirabilis* was analysed by semi-quantitative RT–PCR as mentioned above. The results are shown in Figure 1. Expression of the *acrB* gene in isolates Pm506, Pm609 and Pm805 (ciprofloxacin MICs of >128 mg/L) were 2.8, 2.1 and 3.2 times greater than in the wild-type control strain (PmNC), respectively. These were statistically significant differences ($P < 0.05$). For all of the other isolates, the expression of the *acrB* gene was of the same level as that of the wild-type control strain. The three isolates (Pm506, Pm609 and Pm805) which we hypothesized overexpress the *acrB* gene also had increased MICs of minocycline (>64 versus 8–16 mg/L) and chloramphenicol (>256 versus 4–8 mg/L) compared with the five other fluoroquinolone-resistant isolates (Table 2). A relationship between the other antibiotic susceptibilities (including susceptibilities to erythromycin, clarithromycin, ampicillin, ceftazidime, gentamicin and imipenem) and expression of the *acrB* gene was not recognized.

Table 2. QRDR amino acid mutations of GyrA, GyrB and ParC, and the antibiotic susceptibility in clinical isolates of *P. mirabilis*

Isolate	Amino acid mutations at indicated position in QRDR[a]						MIC (mg/L)										PFGE type
	GyrA		GyrB		ParC												
	Ser-83	Glu-87	Ser-464	Glu-466	Gly-78	Ser-80	CIP	LVX	SPX	MIN	CHL	ERY	CLR	AMP	CAZ	GEN	IPM	
PmNC	–	–	–	–	–	–	≤0.12	≤0.12	≤0.5	8	8	256	256	≤2.0	≤1.0	≤2.0	2	A
Pm701	Ile	–	–	–	–	Arg	4	4	8	16	8	256	256	>64	≤1.0	≤2.0	≤0.5	F
Pm909	Arg	–	Tyr	–	–	Arg	8	16	>32	16	8	256	>256	>64	≤1.0	4	2	H
Pm210	Arg	–	Tyr	–	–	Ile	16	8	>32	8	4	256	>256	≤2.0	≤1.0	≤2.0	2	B
Pm405	Arg	–	Tyr	–	–	Ile	16	8	>32	16	8	>256	>256	≤2.0	≤1.0	≤2.0	1	D
Pm311	Ile	Lys	Phe	–	–	Ile	16	16	>32	16	8	256	>256	>64	≤1.0	≤2.0	1	C
Pm506	Ile	Lys	Phe	–	–	Ile	>128	>64	>32	>64	>256	>256	>256	>64	2	≤2.0	≤0.5	E
Pm609	Ile	Lys	Phe	–	–	Ile	>128	>64	>32	>64	>256	>256	>256	>64	≤1.0	≤2.0	1	E
Pm805	Ile	Lys	Phe	–	–	Ile	>128	>64	>32	>64	>256	>256	>256	16	≤1.0	≤2.0	2	G

CIP, ciprofloxacin; LVX, levofloxacin; SPX, sparfloxacin; MIN, minocycline; CHL, chloramphenicol; ERY, erythromycin; CLR, clarithromycin; AMP, ampicillin; CAZ, ceftazidime; GEN, gentamicin; IPM, imipenem.
[a]Amino acid mutations were identified compared with the sequences of *P. mirabilis* ATCC 29906.

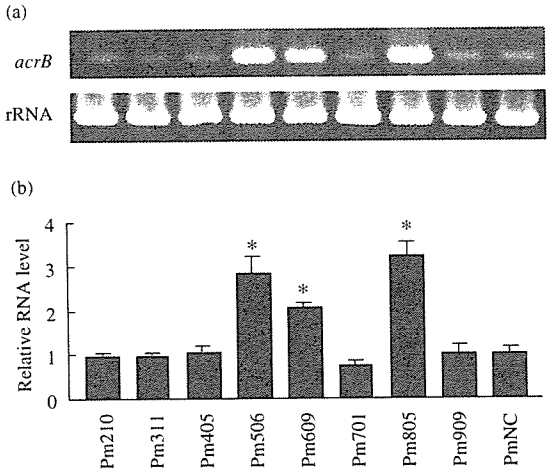

Figure 1. Analysis of expression of *acrB* gene and 16S rRNA in clinical isolates of *P. mirabilis* by semi-quantitative RT–PCR. (a) Representative electrophoresis of RT–PCR product of *acrB* gene and 16S rRNA. Lane 1, Pm210; lane 2, Pm311; lane 3, Pm405; lane 4, Pm506; lane 5, Pm609; lane 6, Pm701; lane 7, Pm805; lane 8, Pm909; lane 9, PmNC. (b) Semi-quantification of *acrB* gene expression—calculated using fluorescence ratio of 16S rRNA (n = 3 for each isolate). *P < 0.05 versus wild-type control strain (PmNC).

Discussion

The mechanisms by which bacteria develop resistance to fluoroquinolones include mutations in the target enzymes (DNA gyrase and topoisomerase IV) and overexpression of endogenous multidrug efflux pumps.[4] The objective of the present study was to investigate the role of amino acid mutations in the target enzymes and the AcrAB efflux pump in clinical isolates of *P. mirabilis* showing resistance to fluoroquinolones.

Isolates Pm506 and Pm609 were both type E, suggesting that the infections caused by *P. mirabilis* in them shared a common origin. Since the seven other isolates were not clonally related there was unlikely to be a common source of infection for them.

Previous studies on amino acid mutations in DNA gyrase and topoisomerase IV associated with fluoroquinolone resistance in *P. mirabilis* have been limited.[5] The study of Weigel *et al.*[5] suggested that a double mutation affecting Ser-83 in GyrA and Ser-80 in ParC was not correlated with fluoroquinolone MICs and that mutation in GyrB is a frequent event in the acquisition of fluoroquinolone resistance. In the present study, mutations in GyrB and ParC occurred in the codons for Ser-464 and Ser-80, respectively, and this is similar to the previous findings.[5] Four of our isolates (Pm311, Pm506, Pm609 and Pm805) having ciprofloxacin MICs of 16 to >128 mg/L had double mutations in GyrA, at Ser-83 and Glu-87, and this was the first time these mutations had been detected in *P. mirabilis*. Previous studies show that a high level of resistance to fluoroquinolones is associated with double mutations in GyrA and an additional mutation in ParC in *E. coli*.[4,13,14] In the present study we did not find a clear relationship between the degree of fluoroquinolone resistance and the number of mutations in GyrA, GyrB and ParC in *P. mirabilis*. However, such a relationship may have been found if a larger number of isolates had been examined.

Recently, it has been demonstrated that DNA gyrase and topoisomerase IV mutations and the efflux pump have a multiplicative effect on the MICs of fluoroquinolones for *E. coli*[6] and *Campylobacter* species.[10] Also, in a previous study, a homologue of the *E. coli* AcrAB efflux pump was identified in *P. mirabilis* and this gene cluster appeared to be responsible for reducing susceptibility to tigecycline and minocycline,[11] but it had yet to be shown that this efflux pump plays a role in the fluoroquinolone resistance of *P. mirabilis*. Thus, using clinical isolates of *P. mirabilis*, we investigated the role of the AcrAB efflux pump in fluoroquinolone resistance by semi-quantifying the transcriptional expression of the *acrB* gene. As indicated in Figure 1, in three isolates (Pm506, Pm609 and Pm805) with ciprofloxacin MICs of >128 mg/L, the degree of expression of the *acrB* gene was 2.8-, 2.1- and 3.2-fold higher, respectively, than that in the wild-type control strain (PmNC). Although we did not look at actual protein levels of the AcrAB efflux pump and did not confirm the role of this pump by inactivating the *acrB* gene via genetic means, overproduction of this pump was consistent with the increased MICs of minocycline and chloramphenicol compared with the other five isolates. Therefore, these results suggest that overproduction of this pump may play a role in fluoroquinolone resistance in clinical isolates of *P. mirabilis*. These three isolates had double mutations in GyrA (corresponding to Ser-83 and Glu-87) in addition to mutations in GyrB and ParC. Thus, overall, our results indicate that two mechanisms—mutations in DNA gyrase and topoisomerase IV and overproduction of the AcrAB efflux pump—might synergistically contribute to the acquisition of a highest level of resistance to fluoroquinolones in clinical isolates of *P. mirabilis*. To our knowledge, this is the first study that has analysed the role of the AcrAB efflux pump in fluoroquinolone-resistant clinical isolates of *P. mirabilis*.

Acknowledgements

We thank Toshio Chida for useful discussions. We did not receive any financial support from third parties.

Transparency declarations

None to declare.

References

1. Rozalski A, Sidorczyk Z, Kotelko K. Potential virulence factors of *Proteus* bacilli. *Microbiol Mol Biol Rev* 1997; **61**: 65–89.

2. de Champs C, Bonnet R, Sirot D *et al.* Clinical relevance of *Proteus mirabilis* in hospital patients: a two year survey. *J Antimicrob Chemother* 2000; **45**: 537–9.

3. Hernandez JR, Martinez-Martinez L, Pascual A *et al.* Trends in the susceptibilities of *Proteus mirabilis* isolates to quinolones. *J Antimicrob Chemother* 2000; **45**: 407–8.

4. Hooper DC. Mechanisms of fluoroquinolone resistance. *Drug Resist Updat* 1999; **2**: 38–55.

5. Weigel LM, Anderson GJ, Tenover FC. DNA gyrase and topoisomerase IV mutations associated with fluoroquinolone resistance in *Proteus mirabilis*. *Antimicrob Agents Chemother* 2002; **46**: 2582–7.

6. Oethinger M, Kern WV, Jellen-Ritter AS *et al.* Ineffectiveness of topoisomerase mutations in mediating clinically significant

fluoroquinolone resistance in *Escherichia coli* in the absence of the AcrAB efflux pump. *Antimicrob Agents Chemother* 2000; **44**: 10–3.

7. Jellen-Ritter AS, Kern WV. Enhanced expression of the multidrug efflux pumps AcrAB and AcrEF associated with insertion element transposition in *Escherichia coli* mutants selected with a fluoroquinolone. *Antimicrob Agents Chemother* 2001; **45**: 1467–72.

8. Baucheron S, Imberechts H, Chaslus-Dancla E *et al.* The AcrB multidrug transporter plays a major role in high-level fluoroquinolone resistance in *Salmonella enterica* serovar Typhimurium phage type DT204. *Microb Drug Resist* 2002; **8**: 281–9.

9. Olliver A, Valle M, Chaslus-Dancla E *et al.* Role of an *acrR* mutation in multidrug resistance of *in vitro*-selected fluoroquinolone-resistant mutants of *Salmonella enterica* serovar Typhimurium. *FEMS Microbiol Lett* 2004; **238**: 267–72.

10. Ge B, McDermott PF, White DG *et al.* Role of efflux pumps and topoisomerase mutations in fluoroquinolone resistance in *Campylobacter jejuni* and *Campylobacter coli*. *Antimicrob Agents Chemother* 2005; **49**: 3347–54.

11. Visalli MA, Murphy E, Projan SJ *et al.* AcrAB multidrug efflux pump is associated with reduced levels of susceptibility to tigecycline (GAR-936) in *Proteus mirabilis*. *Antimicrob Agents Chemother* 2003; **47**: 665–9.

12. National Committee for Clinical Laboratory Standards. *Methods for Dilution Antimicrobial Susceptibility Tests for Bacteria That Grow Aerobically: Approved Standard M7-A6*. NCCLS, Wayne, PA, USA, 2003.

13. Vila J, Ruiz J, Marco F *et al.* Association between double mutation in *gyrA* gene of ciprofloxacin-resistant clinical isolates of *Escherichia coli* and MICs. *Antimicrob Agents Chemother* 1994; **38**: 2477–9.

14. Vila J, Ruiz J, Goni P *et al.* Detection of mutations in *parC* in quinolone-resistant clinical isolates of *Escherichia coli*. *Antimicrob Agents Chemother* 1996; **40**: 491–3.

Cellular Microbiology (2006) 8(10), 1571–1580

doi:10.1111/j.1462-5822.2006.00731.x
First published online 2 May 2006

Bacterial flagellin inhibits T cell receptor-mediated activation of T cells by inducing suppressor of cytokine signalling-1 (SOCS-1)

Shu Okugawa,[1] Shintaro Yanagimoto,[1] Kunihisa Tsukada,[1] Takatoshi Kitazawa,[1] Kazuhiko Koike,[1] Satoshi Kimura,[1] Hiroyuki Nagase,[2] Koich Hirai[2] and Yasuo Ota[1]*

Departments of [1]Infectious Diseases and [2]Bioregulatory Function, Graduate School of Medicine, The University of Tokyo, Tokyo, Japan.

Summary

Flagellin, the structural component of bacterial flagella, is secreted by pathogenic and commensal bacteria, and is recognized by Toll-like receptor (TLR) 5. Flagellin is a common bacterial antigen present on most motile bacteria and is speculated to contribute to the activation of CD4$^+$ T cells in the intestine. However, molecular mechanisms by which flagellin regulate T cell activation remains to be determined. Using Jurkat T cells or human primary T cell, we showed that flagellin stimulation induced tyrosine phosphorylation of TLR5 and activation of both mitogen-activated protein kinases and nuclear factor κB. In addition, stimulation by flagellin did not induce nuclear factor of activated T cells (NFAT) activation, while stimulation via the T cell receptor (TCR) leads to activation of NFAT. However, TCR-mediated NFAT activation and tyrosine phosphorylation of zeta-associated protein 70 (Zap-70) were inhibited in cells pre-stimulated by flagellin. Furthermore, flagellin stimulation induced suppressor of cytokine signalling-1 (SOCS-1), which formed a complex with Zap-70 after stimulation via TCR, and inhibition of SOCS-1 expression by SOCS-1-specific small interfering RNA reinstated TCR-mediated activation of NFAT in cells pre-stimulated with flagellin. These results collectively indicate that bacterial flagellin inhibits TCR-mediated activation of T cells by inducing SOCS-1.

Introduction

Toll-like receptors (TLRs) recognize pathogen-associated molecular patterns (PAMPs) and mediate the production of cytokines necessary for the development of effective immunity (Aderem and Ulevitch, 2000; Brightbill and Modlin, 2000; Means *et al.*, 2000; Medzhitov and Janeway, 2000). Flagellin, the structural component of bacterial flagella, is secreted by pathogenic and commensal bacteria, and is recognized by the innate immune system in organisms as diverse as flies, plants and mammals (Samakovlis *et al.*, 1992; Ciacci-Woolwine *et al.*, 1999; Wyant *et al.*, 1999a,b; Gomez-Gomez and Boller, 2000; McDermott *et al.*, 2000; Steiner *et al.*, 2000). Specifically, flagellin is a common bacterial antigen present on most motile bacteria in the intestine (Winstanley and Morgan, 1997). Flagellin is an extremely potent inducer of cytokine and nitric oxide production (McDermott *et al.*, 2000; Steiner *et al.*, 2000; Eaves-Pyles *et al.*, 2001a,b; Gewirtz *et al.*, 2001a,b; Moors *et al.*, 2001; Ogushi *et al.*, 2001; Sierro *et al.*, 2001). Flagellin induces signalling via TLR5 in a variety of cell types including human and murine monocytes, dendritic cells, epithelial cell lines and TLR5-positive intestinal epithelial cells (Gewirtz *et al.*, 2001a; Hayashi *et al.*, 2001; McSorley *et al.*, 2002a; Mizel and Snipes, 2002; Didierlaurent *et al.*, 2004).

As flagellin is ubiquitously present in the intestine and can be transported across intestinal epithelia by some pathogens (Gewirtz *et al.*, 2001b), it may also contribute to the activation of CD4$^+$ T cells in the intestine (McSorley *et al.*, 2002a). Flagellin enhances the clonal expansion of naive CD4$^+$ T cells *in vivo* and induced production of interferon-γ (IFN-γ) *in vitro* (McSorley *et al.*, 2002a). Marked reactivity against flagellin has also been seen in mesenteric and splenic T cell cultures from colitic animals, and flagellin-specific T cells were able to induce colitis when adoptively transferred into immunodeficient animals (Lodes *et al.*, 2004). Flagellin was also found to be a target of CD4$^+$ T cells during murine *Salmonella typhimurium* infection, and antigenic responses against flagellin are protective in *Salmonella* infections in mice (Cookson and Bevan, 1997; McSorley *et al.*, 2000; 2002b). Given the activity of flagellin as a specific ligand for TLR5, these data provide a potentially important link between adaptive and innate immune responses.

T cells express a relatively small number of TLRs, while macrophages or dendritic cells express wide varieties of TLRs. TLR4 is expressed in murine CD3$^+$ T lymphocytes, and more specifically in particular subsets of

Received 13 October, 2005; revised 8 March, 2006; accepted 9 March, 2006. *For correspondence. E-mail yasuota-tky@umin.ac.jp; Tel. (+81) 3 3815 5411; Fax (+81) 3 5800 8805.

γδ T cells (Matsuguchi *et al.*, 2000; Mokuno *et al.*, 2000). Expression of TLR4, TLR5, TLR7 and TLR8 in regulatory T cell subsets have been reported (Caramalho *et al.*, 2003). Recently, it was also reported that effector memory T cells are stimulated by ligands of TLR5, TLR7 and TLR8 (Caron *et al.*, 2005). In addition, exposure to lipopolysaccharide (LPS) markedly increases activity of regulatory T cells and their proliferative response does not require antigen-presenting cells (APC). This response is augmented by T cell receptor (TCR) triggering, and synergizes with IL-2 stimulation (Caramalho *et al.*, 2003). Furthermore, flagellin synergized with TCR-dependent stimulation [anti-CD3 monoclonal antibody (Ab)] upregulates proliferation and cytokine productions in $CD4^+$ T lymphocytes (Caron *et al.*, 2005). However, the effects of flagellin stimulation in these T cells remain to be determined.

Suppressor of cytokine signalling-1 (SOCS-1) is a member of the protein family regulating cytokine signalling pathways via inhibition of key tyrosine phosphorylation events on cytokine receptors and signalling molecules such as JAK family members. SOCS-1 interacts with JAK tyrosine kinases and inhibits kinase activity, thereby suppressing cytokine signal transduction (Yasukawa *et al.*, 2000; Kubo *et al.*, 2003). Furthermore, SOCS-1 expression is rapidly induced by LPS and negatively regulates LPS signalling (Crespo *et al.*, 2000; Crespo *et al.*, 2002). In SOCS-$1^{-/-}$ mice, innate immunity is strongly enhanced, probably due to hypersensitivity of SOCS-$1^{-/-}$ mice to IFN-γ (Alexander *et al.*, 1999). SOCS-1 has been implicated in the hypo-responsiveness to cytokines, such as IFN-γ, after exposure of LPS to macrophages (Crespo *et al.*, 2002). SOCS-1-deficient mice are more sensitive to LPS shock than their wild-type littermates, and SOCS-1 overexpression suppresses LPS-induced inhibitory kappa B (I-κB) phosphorylation and NF-κB transcriptional activity (Kinjyo *et al.*, 2002; Nakagawa *et al.*, 2002). However, it was recently reported that SOCS proteins induced by TLR stimulation limit the extent of TLR signalling by inhibiting type I interferon signalling but not the direct NF-κB pathway via TLR (Baetz *et al.*, 2004; Gingras *et al.*, 2004). To our knowledge, no reports on whether SOCS proteins are induced by flagellin stimulation and whether they regulate TLR5-mediated signal transduction cascades have been published.

It was reported that a prior exposure to flagellin results in a subsequent state of flagellin tolerance in Jurkat T cells (Mizel and Snipes, 2002). In this study we examined whether Jurkat T cells or human primary T cells were activated by flagellin and whether pre-treatment of flagellin modulated TCR-mediated activation with particular focus on the role of SOCS-1.

Results

TLR5 surface expression in Jurkat T cells and TLR5 tyrosine phosphorylation by flagellin

To examine whether Jurkat T cells expressed TLR5 protein on the cell surface, we analysed surface expressions of TLR5 in Jurkat T cells by FACS (Mizel and Snipes, 2002). As shown in Fig. 1A, Jurkat T cells express TLR5 at the cell surface. We next examined whether flagellin itself induced tyrosine phosphorylation of TLR5. As shown in Fig. 1B, flagellin stimulation induced tyrosine phosphorylation of TLR5 within 1 min. To confirm that tyrosine-phosphorylation of TLR5 was specifically induced by flagellin stimulation, we examined whether stimulation

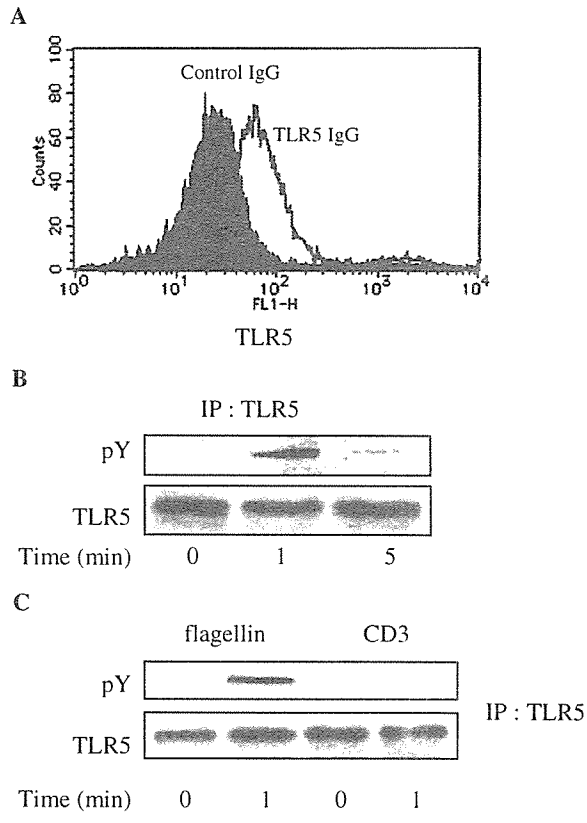

Fig. 1. TLR5 is expressed at the cell surface of Jurkat T cells and is tyrosine-phosphorylated by flagellin stimulation.
A. Jurkat T cells were stained with anti-TLR5 antibody (Ab) and FITC-conjugated donkey anti-goat secondary Ab. Cells expressed with TLR5 were examined by FACS analysis.
B. Jurkat T cells were stimulated with 10 ng ml^{-1} flagellin for the indicated times. Cell lysates were immunoprecipitated (IP) with TLR5 Ab and probed with anti-phosphotyrosine Ab, 4G10 (top), or anti-TLR5 (bottom).
C. Jurkat T cells were stimulated with 10 ng ml^{-1} flagellin or 1 μg ml^{-1} anti-CD3 Ab (UCHT1) for 1 min. Cell lysates were immunoprecipitated with TLR5 Ab and probed with anti-phosphotyrosine Ab, 4G10 (top), or anti-TLR5 (bottom).

